

Grant-free Random Access with Self-conjugating Metasurfaces

Davide Dardari, *Senior Member, IEEE*, Marina Lotti, *Student Member, IEEE*,
Nicoló Decarli, *Member, IEEE*, Gianni Pasolini, *Member, IEEE*

Abstract

Recently, grant-free random access schemes have received significant attention in the scientific community as a solution for extremely low-latency massive communications in new industrial Internet-of-things (IIoT) and digital twins applications. Unfortunately, the adoption of such schemes in the mmWave and THz bands is challenging because massive antenna arrays are needed to counteract the high path loss and provide massive access with consequent significant signaling overhead for channel estimation and slow beam alignment procedures between the base station (BS) and user equipments (UEs), which are in contrast to the ultra-low-latency requirement, as well as to the need for low hardware complexity and energy consumption. In this paper, we propose the adoption of a self-conjugating metasurface (SCM) at the UE side, where the signal sent by the BS is reflected after being conjugated and phase-modulated according to the UE data. Then, a novel grant-free random access protocol is presented capable to detect new UEs and establish parallel multiple-input multiple-output (MIMO) uplink communications with almost zero latency and jitter. This is done in a blind way without the need for RF/ADC chains at the UE side as well as without explicit channel estimation and time-consuming beam alignment schemes.

Index Terms

Self-conjugating metasurfaces; Grant-free random access; MIMO; Retro-directive backscattering; Intelligent surfaces.

I. INTRODUCTION

Future wireless networks are expected to satisfy very challenging requirements in terms of data rate, latency, energy efficiency, and nodes density, in order to enhance the performance of existing massive Machine Type Communication (mMTC) applications and enable new ones [1]. Among them, the creation of digital twin worlds perfectly intertwined with physical objects in industrial Internet-of-things (IIoT) environments, is certainly one of the most challenging [2], [3]. Here, ultra-low latency ($< 100 \mu s$), low jitter ($\approx 1 - 2 \mu s$), ultra-massive access (10 sensors/m^2), high energy efficiency, and low complexity, often must be satisfied simultaneously. The exploitation of high frequencies in the mmWave and THz bands is one direction of investigation to gain more bandwidth, which however requires massive antenna arrays with very narrow beams (also at the user side) to compensate for the high path loss and obtain better spatial filtering to reduce the interference between users that are using the same radio resource. However, massive antenna arrays also introduce new issues due to signaling overhead (e.g., for channel estimation), high hardware complexity, increased power consumption, and slow beamforming and alignment procedures, which are in contrast with the low-latency requirement and the possibility to embed wireless devices into low-cost, small and low-energy sensors (e.g., exploiting energy harvesting techniques [4]). In addition, in mMTCs the generated traffic is often sporadic, random, and characterized by the transmission of short packets. Under these conditions, to keep the access latency at extremely low values, any coordination action from the BS, such as scheduling, synchronization, or retransmission, is typically avoided in favor of grant-free access schemes [5]. In this context, channel state information (CSI) estimation becomes extremely challenging, especially in MIMO systems. In fact, channel estimation typically relies on the assumption that devices are active for a long period so that long preambles (pilot symbols) can be allocated without a significant loss in efficiency. Vice versa, in mMTCs the CSI has to be estimated on a one-shot basis with an extremely limited space available for pilot symbols allocation. For instance, the initial beam alignment procedure (i.e., the CSI estimation) requires, in general, that both the BS and UE test all possible pairs of angles before the UE could be visible to the BS and the communication established [6]. These approaches either involve some computational effort on both sides, which affects hardware complexity and power consumption, or long training data/search time, which increases latency. Clearly, these problems are emphasized when the number of antennas is high. Moreover, at high frequencies, such as sub-THz/THz, technological

constraints place several limitations on the flexibility in processing the signal sent/received by each individual antenna element, thus reducing the set of affordable solutions (digital bottleneck). Therefore, it is of paramount importance to study solutions enabling ultra-low latency grant-free MIMO random access using low-complexity, low-power devices at mmWave and beyond, characterized by limited or no overhead associated with CSI estimation and user detection.

Recently, intelligent metasurfaces have attracted a lot of interest in the research community as a technology to realize extremely (electrically) large antennas, namely large intelligent surfaces (LISs), and reconfigurable intelligent surfaces (RISs) capable to modify the way the electromagnetic (EM) waves propagate in the environment with zero additional latency and low-consumption [7]–[10]. Typically, RISs have been proposed to cope with coverage extension in non line-of-sight (NLOS) channel conditions [11]–[14]. Other recent uses consider the possibility for the RIS to embed opportunistically some information while reflecting a signal from a BS towards the intended user(s) [15]–[17]. This is done through the adoption of backscatter modulation [18], [19]. Another interesting direction of research to overcome the digital bottleneck is to move some basic processing functionalities directly to the intelligent metasurface, that is, at the EM level. This is expected to bring advantages in terms of latency, power consumption, size, and complexity reduction, especially at mmWave and THz, with respect to the digital implementation counterpart [20], [21]. One question is therefore whether intelligent metasurfaces can help in finding solutions to the above-mentioned challenges for grant-free MIMO random access.

For the purposes of this paper, we focus on a particular type of RIS, usually denoted as self-conjugating metasurface (SCM). SCMs are specific surfaces capable of reflecting an EM wave, typically employed to obtain the retro-directivity effect [22], whose complex envelope is the conjugate of the envelope of the impinging EM wave. Retro-directivity has been investigated for a long time in different contexts such as radar, wireless power transfer, collision avoidance systems, microwave imaging or detection, RFID systems, and remote information retrieval from sensors. In [23], an SCM is used to continuously track a single user in a fast time-variant channel. However, to the Authors' best knowledge, its use for efficient wireless communications has been little studied [22] and has never been considered for grant-free random access MIMO systems, as we do in this work. Specifically, in this paper, we exploit the properties of SCMs to design an almost zero-latency grant-free random access MIMO scheme with asynchronous UEs. One important peculiarity of the proposed scheme is that it does not need any overhead for

CSI estimation and any ADC and baseband processing at UE side, thus allowing the efficient transmission of short packets in mMTC applications with low-complexity devices.

A. Related Works

Massive random access has been a hot topic for many years and several approaches have been proposed. For a general overview, the reader can refer to the survey in [5]. Grant-free massive random access schemes have to deal not only with inter-user interference but also with the problem of detecting the presence of active users and estimating the channel [24], [25]. Various solutions have been proposed. For instance, coded random access protocols allow an increased level of reliability thanks to the joint exploitation of interference cancellation and coding techniques on top of classical ALOHA-based random access protocols [26]. As an example, explicit preamble transmission is avoided in the coded random access scheme investigated in [27] by assigning to each user a unique channel access pattern which is used to embed user identities and facilitate the detection. In any case, coded random access relies on the transmission of some replicas of the same packet in order to perform interference cancellation that might deny the achievement of sub-ms latency. In [28], a single-antenna massive access scheme is proposed where the device ID is embedded in the sequence used to spread the signal, thus eliminating the explicit transmission of the ID, and the channel estimation is avoided thanks to a non-coherent multi-user detector aided by an unsupervised machine learning algorithm. The main drawbacks of the scheme are the increased bandwidth due to spreading and the fact that it is tailored to single-antenna configurations.

Massive MIMO has demonstrated the possibility to reduce the effect of inter-user interference to any level provided that the number of antennas at the BS grows indefinitely under typical channel characteristics [29]. This allows communication with a large number of users simultaneously sharing the same radio resource. In [24], an asymptotic regime analysis of user activity detection and channel estimation is carried out as the number of antennas at the BS becomes massive. Specifically, the authors quantify the performance of user activity detection and channel estimation when randomly generated non-orthogonal pilot sequences are assigned to each device. They show that the user activity detection error can be arbitrarily small when increasing the number of antennas, whereas the channel estimation error and the overhead for pilots remain the main bottleneck. The rich dimensionality of the sparse angular domain MIMO channel is exploited in [30] to design an uncoupled slotted data transmission scheme for unsourced random

access. The similarity of the angular transmission pattern implied in the slot-wise reconstructed channels allows the design of a clustering-based decoder combining message sequences across slots. The work in [31] combines instantaneous CSI with long-term statistical CSI in a massive MIMO context assuming that channel singular vectors are known and constant over a long term. The beamforming design is shown to improve the mean signal-to-noise ratio (SNR) and reduce its standard deviation while keeping the latency below 0.5 ms, and hence suitable for ultra-reliable low-latency communications (URLLC) applications. Finally, in [32], a joint active user detection and channel estimation scheme in support of massive access is proposed with the adoption of a multi-panel massive MIMO in a cellular IIoT scenario working at mmWave and THz. The scheme takes advantage of the sparsity of active users to successfully exploit compressed sensing techniques.

Despite the rich literature on the subject, to the authors' knowledge, no solutions have been proposed ensuring grant-free random access with ultra-low latency (e.g., $< 100 \mu\text{s}$) and jitter, no overhead for CSI estimation, in a MIMO mMTC scenario using ultra-low complexity devices.

B. Our Contribution

In this paper, we introduce a MIMO scheme which overcomes the previous limitations and allows zero-latency grant-free access to asynchronous MIMO devices equipped with SCMs. The main idea is to have different parallel tasks running at the BS that generate proper sounding signals and process the signal received by the BS antenna array. In order to detect new users, a dedicated *Scouting Task* is always running on a channel subspace orthogonal to those used by the already active links. In particular, the Scouting Task jointly exploits retro-directivity and the backscatter communication of a modulating SCM at the UE side, where the signal sent by the BS is reflected (backscattered) after being conjugated and phase-modulated according to the user's data directly at EM level (*retro-directive backscattering*). It will be shown that operating in this way, the BS and the UE can establish a MIMO uplink communication without any computational effort at the UE side nor any signaling. More precisely, thanks to the methodology introduced in this paper, the BS is able to derive the optimal beamforming vector (precoding vector), which corresponds to the top eigenvector of the BS-UE round-trip channel, by iterating with the SCM and making use of a modified *Power Method* for the eigenvectors estimation [33]. This is done blindly in an almost optimal manner, without the need for either the CSI estimation or time-consuming beam alignment schemes. Every time a new user is detected, the BS activates

a dedicated task, named *Communication Task*, which makes use of the beamforming vector estimated by the Scouting Task addressing a channel subspace orthogonal to those already under exploitation by the Communication Tasks serving the other currently active users. The result is a scheme where complexity grows linearly with the number of UEs and is capable of managing asynchronous random transmissions of packets of any size without the explicit estimation of the multi-user MIMO channel, thus ensuring an almost zero latency and no jitter independently of the number of UEs.

We further characterize analytically the convergence behavior of the Scouting Task taking into account the noise generated by the SCM and the BS. Numerical results put in evidence that almost optimal beamforming can be achieved within the transmission of a few symbols at the BS and UE sides, without any processing at the UE. The increased path loss due to the backscatter nature of the communication link can be easily compensated by increasing the number of antennas at the UE without additional processing. The adoption of the SCM at the UE allows an extremely low-complexity and low-power design of the UE because no ADC chains are needed. It is worth remarking that in this case, the metasurface is part of the UE, not an additional element deployed in the environment like in most of the RIS-based scenarios investigated in the literature.

The rest of the paper is structured as follows: In Sec. II, a brief overview of SCMs is given and the strategy to exploit them to transmit data is proposed. The illustration of the working principle of SCM-based communication is given in Sec. III. The proposed algorithms for random access are described in Sec. IV and the convergence analysis is presented in Sec. V. Numerical results are illustrated in Sec. VI, whereas the conclusions are drawn in Sec. VII.

C. Notation and Definitions

Boldface lower-case letters are vectors (e.g., \mathbf{x}), whereas boldface capital letters are matrices (e.g., \mathbf{H}), where \mathbf{I}_N is the identity matrix of size N , and $\|\mathbf{x}\|$ represents the Euclidean norm of vector \mathbf{x} . \mathbf{H}^T and \mathbf{H}^\dagger indicate, respectively, the transpose and the conjugate transpose operators applied to matrix \mathbf{H} , whereas $\|\mathbf{H}\|_F$ denotes the Frobenius norm of \mathbf{H} . The notation $x \sim \mathcal{CN}(m, \sigma^2)$ indicates a complex circular symmetric Gaussian random variable (RV) with mean m and variance σ^2 , whereas $\mathbf{x} \sim \mathcal{CN}(\mathbf{m}, \mathbf{C})$ denotes a complex Gaussian random vector with mean \mathbf{m} and covariance matrix \mathbf{C} .

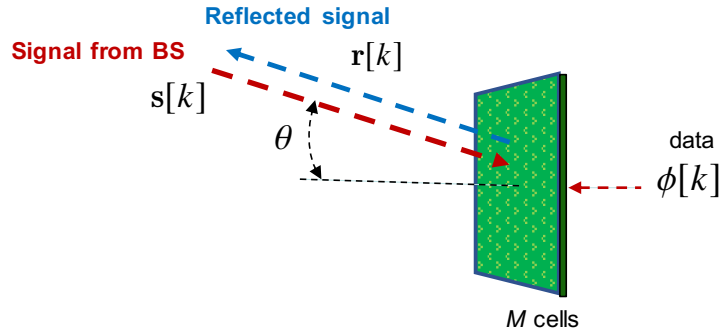


Fig. 1. Modulating self-conjugating metasurface (SCM) at the UE side.

II. MODULATING SELF-CONJUGATING METASURFACES

With reference to Fig. 1, consider a metasurface (or an antenna array), namely SCM, composed of M elements (cells) and a narrowband impinging signal $\mathbf{s}[k] = [s_1[k], s_2[k], \dots, s_M[k]]^T$ of bandwidth W , where $s_m[k]$ represents the equivalent low-pass discrete-time version of the signal at the input of the m th cell at discrete time k . A SCM is characterized by the property such that the backscattered equivalent low-pass signal is the conjugate of the input signal [22], that is,

$$\mathbf{r}[k] = g \mathbf{s}^*[k] + g \boldsymbol{\eta}^*[k] \quad (1)$$

where $\boldsymbol{\eta}[k] \in \mathbb{C}^{M \times 1}$ is the additive white Gaussian noise (AWGN), with $\boldsymbol{\eta}[k] \sim \mathcal{CN}(\mathbf{0}, \sigma_\eta^2 \mathbf{I}_M)$, and g is the gain of the cell ($g < 1$ if it is passive). Note that $\sigma_\eta^2 = \kappa T_0 F_{\text{SCM}} W$, being κ the Boltzmann constant, $T_0 = 290$ K, and F_{SCM} the cell's noise figure [34]–[37].

An interesting property of an SCM is *retro-directivity* [22]. In fact, when it is illuminated by a plane wave with incident angle θ , ideally the signal is backscattered towards the same angle. For example, if an uniform linear array (ULA)-like SCM with inter-element spacing Δ is considered, an impinging plane wave with incident angle θ can be generically expressed as $s_m[k] = A e^{j \frac{2\pi}{\lambda} m \Delta \sin(\theta)}$, for $m = 1, 2, \dots, M$, where λ is the wavelength and A is a generic complex constant. According to (1) and neglecting the noise term, the backscattered signal is $r_m[k] = g s_m^*[k] = g A^* e^{j \frac{2\pi}{\lambda} m \Delta \sin(-\theta)}$, for $m = 1, 2, \dots, M$, which corresponds to a plane wave reflected back toward the same direction θ .

The most common approach to realize the self-conjugating property is through heterodyne mixing of the incoming wave, centered at frequency f_0 , with a locally generated sinusoid oscillating at $2f_0$. One of the earliest demonstrations of the retro-directivity property is that one

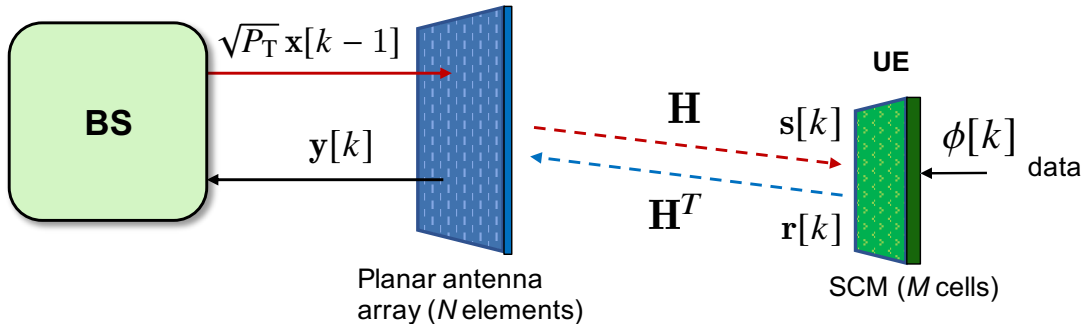


Fig. 2. Principle scheme of a SCM-based MIMO communication.

described in [38], where an antenna array with 8 slot antennas, each of which was connected to a Schottky diode performing heterodyne mixing was realized and tested. Another relatively simple solution is proposed in [39], in which active split-ring resonators loaded with varactor diodes are demonstrated to act as phase-conjugating elements when pumped with a signal at frequency $2f_0$. In addition to the previous active solutions, also low-complexity passive retro-directive metasurfaces have been recently realized (in this case $g < 1$). By properly engineering the surface impedance according to a supercell design periodicity that is greater than the wavelength λ , it is possible to reflect the incident wave in a direction other than specular. This principle is exploited, for instance, in [40] to realize a metasurface that exhibits a high level of retro-directivity for several angles of incidence.

Suppose, now, that the metasurface not only performs the conjugation and (possible) amplification of the received signal but also introduces, in each k th symbol interval, a phase shift $\phi[k]$ (the same for all cells) that incorporates the information to be transmitted by the UE in that interval (see Fig. 1). As a consequence, the vector of the backscattered signal becomes

$$\mathbf{r}[k] = g e^{j\phi[k]} \mathbf{z}^*[k] \quad (2)$$

where $\mathbf{z}[k] = \mathbf{s}[k] + \boldsymbol{\eta}[k]$. The conjugation operation will be exploited by the algorithm proposed in the next sections. Since the phase $\phi[k]$ affects all cells of the metasurface, it does not compromise the retro-directivity behavior as the common phase term can be absorbed by the constant A . Moreover, the implementation of the modulated SCM does not require RF/ADC chains as data directly modulates the phase sequence $\{\phi[k]\}$, thus allowing a low-cost, low-complexity, low-energy consumption multi-antenna device.

III. WORKING PRINCIPLE OF SCM-BASED MIMO COMMUNICATION

In this section, we start with the single-user uplink scenario, shown in Fig. 2, with the purpose to illustrate how data can be transmitted from an SCM-based UE to the BS. In particular, we consider a BS, equipped with an antenna array of N elements, capable of full-duplex narrow-band transmission with bandwidth W . The time interval T between time instants $k - 1$ and k is in the order of $1/W$.¹ The UE is realized according to the scheme described in Sec. II, thus incorporating an SCM-based antenna composed of M cells. Let $\sqrt{P_T} \mathbf{x}[k - 1] \in \mathbb{C}^{N \times 1}$ be the vector containing the signal transmitted by the N elements of the BS's antenna array during the k th time interval $[(k - 1)T, kT]$, where P_T is the transmitted power and $\mathbf{x}[k - 1]$ is a unitary norm beamforming vector, i.e., the precoding vector designed to steer the beam toward the UE according to the scheme proposed in Sec. IV. The transmitted signal is received and retro-directed by the UE during the time interval k , then collected by the BS. Here, we assume symbol-level synchronization between the UE and the BS.²

The signal received by the UE in the k th time interval is

$$\mathbf{z}[k] = \sqrt{P_T} \mathbf{H} \mathbf{x}[k - 1] + \boldsymbol{\eta}[k] \quad (3)$$

where $\mathbf{H} \in \mathbb{C}^{M \times N}$ denotes the channel matrix. At the UE, information data is associated with the phase sequence $\{\phi[k]\}_{k=1}^K$, forming a packet of length K symbols, according to any phase-based signaling scheme (e.g., BPSK). Without loss of generality, we consider that all transmitted packets have the same length K , even though packets with different lengths can be easily managed by the scheme proposed in this paper without any change. The signal backscattered by the UE, according to (2), is

$$\mathbf{r}[k] = g e^{j\phi[k]} \mathbf{z}^*[k] = \sqrt{P_T} g e^{j\phi[k]} \mathbf{H}^* \mathbf{x}^*[k - 1] + g \boldsymbol{\eta}^*[k] \quad (4)$$

being $\phi[k]$ the phase associated to the k th data symbol of the transmitted packet. At the BS side, the received signal at time interval k is

$$\mathbf{y}[k] = \sqrt{P_T} g e^{j\phi[k]} \mathbf{H}^T \mathbf{H}^* \mathbf{x}^*[k - 1] + g \mathbf{H}^T \boldsymbol{\eta}^*[k] + \mathbf{w}[k] \quad (5)$$

¹When describing the transmitted signal and the signal received/retro-directed by the UE, time instants k should be intended as intervals. Sampling is operated at the BS after standard matched filter processing of the signal in the last symbol interval of duration T .

²The analysis of schemes at the BS capable of synchronizing with the local clock of the UE is outside the scope of this paper, and it will be the topic of future works.

where $\mathbf{w}[k] \sim \mathcal{CN}(\mathbf{0}, \sigma_w^2 \mathbf{I}_N)$ is the AWGN at the receiver, $\sigma_w^2 = \kappa T_0 F_{\text{BS}} W$, being F_{BS} the BS' noise figure. The noise term $\mathbf{w}[k]$ might also include any clutter backscattered by the surrounding environment whose specific characterization depends on the environment itself. For further convenience, we can rewrite (5) as

$$\mathbf{y}[k] = \sqrt{P_T} e^{j\phi[k]} \mathbf{A}^* \mathbf{x}^*[k-1] + \mathbf{n}^*[k] \quad (6)$$

where we have defined $\mathbf{A} = g \mathbf{H}^\dagger \mathbf{H} \in \mathbb{C}^{N \times N}$, $\mathbf{n}^*[k] = g \mathbf{H}^T \boldsymbol{\eta}^*[k] + \mathbf{w}[k] \sim \mathcal{CN}(\mathbf{0}, \sigma_w^2 \mathbf{I}_N + \sigma_\eta^2 \mathbf{A}^*)$, which includes all the noise terms. Note that, because of the conjugation operated by the SCM, \mathbf{A} is not the round-trip channel which is given, instead, by $g \mathbf{H}^T \mathbf{H}$. For this reason, we refer to it as the *modified round-trip channel*.

Denote with λ_j the j th eigenvalue of \mathbf{A} , where $\lambda_1 \geq \lambda_2 \geq \dots \geq \lambda_N$, and \mathbf{v}_j is the corresponding eigenvector (direction). As a consequence, vector $\mathbf{n}[k]$ can be decomposed as

$$\mathbf{n}[k] = \sum_{j=1}^N n_j[k] \mathbf{v}_j \quad (7)$$

where $n_j[k]$ is the projection of $\mathbf{n}[k]$ onto the j th direction \mathbf{v}_j , and $n_j \sim \mathcal{CN}(0, \sigma_j^2)$, with $\sigma_j^2 = \sigma_w^2 + \lambda_j \sigma_\eta^2$. In a typical practical setting, the modified round-trip channel gain $\|\mathbf{A}\|_F^2$ is much less than one, then the noise component $\mathbf{w}[k]$ becomes the dominant term in $\mathbf{n}[k]$ and hence we can write with good approximation $\sigma_j^2 = \sigma^2, \forall j$, with $\sigma^2 \simeq \sigma_w^2$ (isotropic noise). Interestingly, thanks to the conjugating operation at the user's SCM, the eigenvectors of \mathbf{A} correspond to the left-eigenvectors of the MIMO channel \mathbf{H} , then the estimation of the optimum beamforming vector $\mathbf{x}[k]$ is equivalent to computing the top-eigenvector \mathbf{v}_1 of the modified round-trip channel \mathbf{A} at the BS without requiring any processing at UE side, as it will be evident in Sec. IV.

Information data can be extracted by the BS at each time interval by forming the decision variable $u[k]$ through the correlation of the received vector $\mathbf{y}[k]$ with the complex conjugate of the beamforming vector $\mathbf{x}^\dagger[k-1]$

$$u[k] = \mathbf{x}[k-1]^\dagger \mathbf{y}^*[k]. \quad (8)$$

In particular, assuming a perfect estimation of the beamforming vector \mathbf{v}_1 is available, then

$\mathbf{x}[k-1] = \mathbf{v}_1$ and

$$u[k] = \sqrt{P_T} e^{-j\phi[k]} \mathbf{v}_1^\dagger \mathbf{A} \mathbf{v}_1 + \mathbf{v}_1^\dagger \mathbf{n}[k] = \sqrt{P_T} \lambda_1 e^{-j\phi[k]} + n_1[k] \quad (9)$$

with $n_1 \sim \mathcal{CN}(0, \sigma^2)$. Starting from $u[k]$, a decision on the phase $\phi[k]$ can be made by taking its argument, i.e., $\hat{\phi}[k] = \text{demodulation}(-\arg u[k])$, where $\text{demodulation}(\cdot)$ is the data detection function which depends on the particular signaling scheme considered. Without loss of generality, in our numerical results, we will consider the BPSK scheme. The corresponding SNR at the decision device is

$$\text{SNR} = \frac{P_T \lambda_1^2}{\sigma^2}. \quad (10)$$

It is worth noticing that when the channel has rank $r = 1$, the resulting communication scheme is capacity-optimal provided that an accurate estimation of the beamforming vector \mathbf{v}_1 is available. When $r > 1$, the scheme is not capacity-optimal because the SCM is intrinsically single-layer so that only one out of the r potential data streams, which could be established between the BS and the UE, is exploited. However, it corresponds to the optimal single-layer beamforming scheme in the SNR maximization sense also providing the maximum diversity gain [41].

It is interesting to analyze the SNR in free-space condition assuming the BS and the SCM are in paraxial configuration at distance d . In this case, the SNR in (10) becomes

$$\text{SNR} = \frac{P_T g^2 N^2 M^2 G_{\text{BS}}^2 G_{\text{SCM}}^2 \lambda^4}{\sigma^2 (4\pi d)^4} \quad (11)$$

where G_{BS} and G_{SCM} are the gain of the elements of the BS's antenna and the SCM's cell, respectively. The last equation shows that, due to the backscattering nature of the communication, the path loss increases with the distance to the power of four, as happens with radio frequency identification (RFID) systems based on backscatter modulation [18]. On the other hand, such large path loss can be easily compensated by increasing the number of antenna elements N and M at the BS and UE, respectively.

Now, in order to establish the single-layer optimal communication between the UE and the BS, the main problem to be solved is the fast detection of a new user and the fast and accurate estimation of the beamforming vector \mathbf{v}_1 , especially in a multi-user MIMO scenario. In the next section, a fast and blind (i.e., without CSI estimation) scheme for joint eigenvectors estimation and multi-user communication is presented.

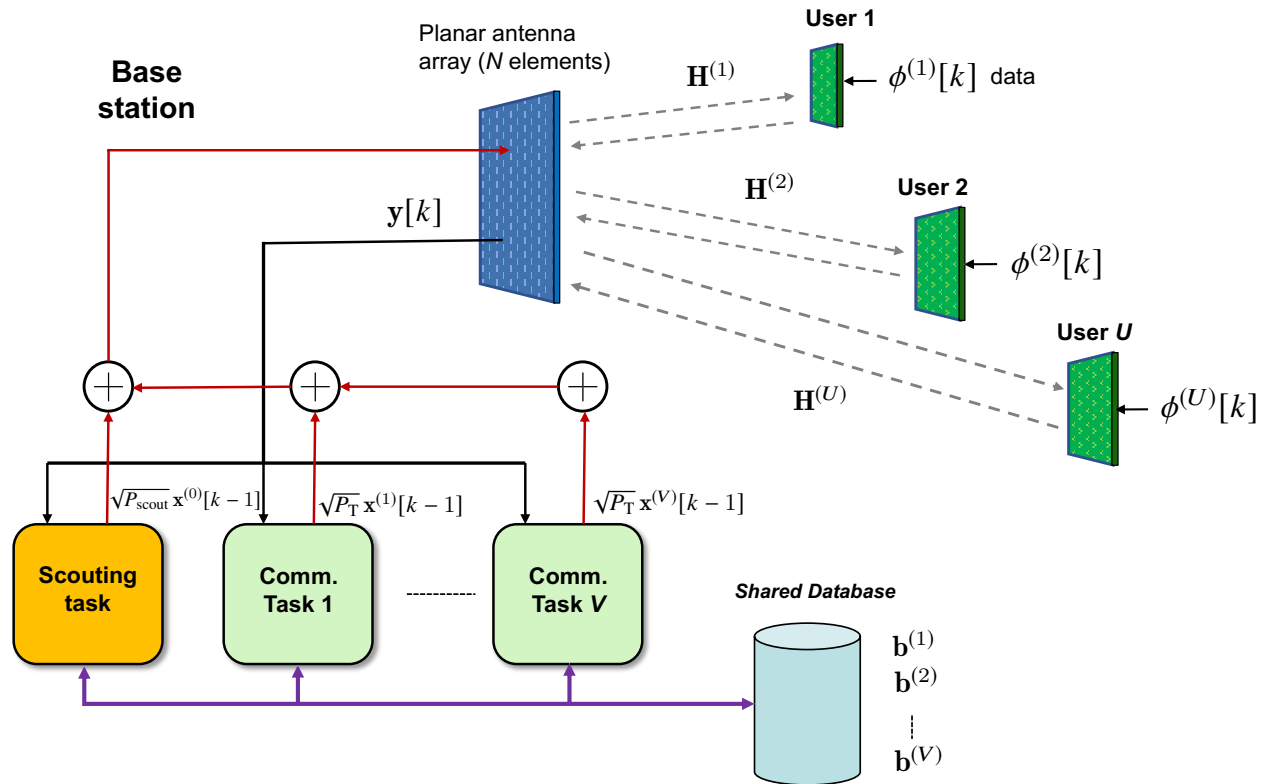


Fig. 3. Scheme of the proposed grant-free MIMO access based on SCMs.

IV. GRANT-FREE RANDOM ACCESS USING MIMO SCMS

Consider a scenario in which a large number of asynchronous UEs deployed in the environment generate packets randomly. We consider the worst-case situation where each packet is generated by a distinct UE located at a different location so that the reception of each packet requires the fast detection of the new UE and the fast estimation of the beamforming vector at the BS without any a priori information. For this reason, in what follows we will interchange freely the terms packets and UEs. Note that in such a scenario, all the approaches relying on statistical/long-term CSI and/or UEs activity pattern estimation are highly inefficient or not applicable (e.g., [31]).

Suppose that, at the generic time interval, there are U asynchronous active (i.e., transmitting) UEs. Denote with $\mathbf{H}^{(1)}, \mathbf{H}^{(2)}, \dots, \mathbf{H}^{(U)} \in \mathbb{C}^{M \times N}$ the channel matrices related to the U links between the BS and the active UEs. For further convenience, we define the corresponding modified round-trip channels $\mathbf{A}^{(u)} = g \left(\mathbf{H}^{(u)} \right)^\dagger \mathbf{H}^{(u)} \in \mathbb{C}^{N \times N}$, for $u = 1, 2, \dots, U$. In addition, we denote with $\mathbf{v}_i^{(u)}$ and $\lambda_i^{(u)}$, respectively, the i th eigenvector and eigenvalue of $\mathbf{A}^{(u)}$, with $i = 1, 2, \dots, r^{(u)}$, where $r^{(u)} = \text{rank} \left(\mathbf{A}^{(u)} \right)$.

The main idea of the proposed grant-free MIMO access scheme is sketched in Fig. 3 and described in the following. The BS has several tasks running in parallel. In particular, one task, namely *Scouting Task*, is always active and its purpose is to discover any newly transmitted packet from a new active UEs and estimate the corresponding, possibly optimal, beamforming vector at the BS. Once a new packet has been detected, the estimated beamforming vector, namely $\mathbf{b}^{(v)}$, is added to a *Shared Database*, containing all the estimated beamforming vectors of the packets currently under decoding. In addition, a dedicated task, denoted to as *Communication Task*, is instantiated and associated to the new packet in charge of decoding it until its end. When the packet is over, i.e., the UE stops transmitting, the associated Communication Task is terminated and the corresponding beamforming vector is removed from the Shared Database. As it will be explained later, if $r^{(u)} > 1$, then the same packet transmitted by the u th UE might be decoded using different orthogonal beamforming vectors, each of them associated with a different eigenvalue of $\mathbf{A}^{(u)}$. As a consequence, the size of the Shared Database, and then the number V of instantiated Communication Tasks, might be in general equal or larger than the number U of currently active UEs, that is, $V \geq U$. Denote with $u = f(v)$ the function that maps the packet under decoding by the v th Communication Task with the index u of the UE that generated it.

According to the scheme in Fig. 3, the Scouting Task and the V Communication Tasks generate, respectively, the beamforming vectors $\sqrt{P_{\text{scout}}} \mathbf{x}^{(0)}[k-1]$ and $\sqrt{P^{(v)}} \mathbf{x}^{(v)}[k-1] = \sqrt{P^{(v)}} \mathbf{b}^{(v)}$, $v = 1, 2, \dots, V$, which are summed up to form the actual transmitted vector $\mathbf{x}[k-1]$ at time $k-1$, that is,

$$\mathbf{x}[k-1] = \sum_{v=0}^V \sqrt{P^{(v)}} \mathbf{x}^{(v)}[k-1] \quad (12)$$

where $P^{(0)} = P_{\text{scout}}$ and $\mathbf{x}^{(0)}[k-1]$ are, respectively, the transmitted power and the current beamforming vector used by the Scouting Task. Without loss of generality, we assume that all the Communication Tasks transmit with the same power P_T , so $P^{(v)} = P_T$, $v = 1, 2, \dots, V$. The signal received by the SCM of the u th UE during the k th transmission interval is

$$\mathbf{z}^{(u)}[k] = \mathbf{H}^{(u)} \mathbf{x}[k-1] + \boldsymbol{\eta}^{(u)}[k] = \mathbf{H}^{(u)} \sum_{l=0}^V \sqrt{P^{(l)}} \mathbf{x}^{(l)}[k-1] + \boldsymbol{\eta}^{(u)}[k] \quad (13)$$

where $\boldsymbol{\eta}^{(u)}[k] \sim \mathcal{CN}(\mathbf{0}, \sigma_{\eta}^2 \mathbf{I}_M)$ is the noise of the SCM of the u th UE. In (13), $\mathbf{H}^{(u)}$ represents the channel matrix between the BS and the possibly new UE under scouting. Therefore $u \in \mathcal{U}$,

Algorithm 1: Algorithm of the Scouting Task.

Initialization: generate a guess unitary norm beamforming vector $\mathbf{x}^{(0)}[0]$; $V = 0$;
for $k = 1, \dots, \infty$ **do**
 If the Shared Database has been updated, then generate a random unitary norm vector $\mathbf{x}^{(0)}[k-1]$ orthogonal to \mathbf{B} //
 transmit: $\sqrt{P_{\text{scout}}}\mathbf{x}^{(0)}[k-1]$ //
 receive: $\mathbf{y}[k]$ //
 $\hat{\mathbf{y}}[k] = \text{orthogonalize}(\mathbf{y}[k], \mathbf{B})$ //
 $\mathbf{x}^{(0)}[k] = (\hat{\mathbf{y}}[k])^* / \|\hat{\mathbf{y}}[k]\|$ // beamforming vector update
 $\gamma[k] = \|\hat{\mathbf{y}}[k]\|^2 / \sigma^2$ // SNR computation
 If $\gamma[k] > \gamma_{\text{dec}}$ and $\gamma[k] / \gamma[k-1] < \gamma_{\Delta}$, then a new packet has been detected, $V = V + 1$, a new dedicated Communication Task is allocated using $\mathbf{x}^{(0)}[k]$ as beamforming vector, and $\mathbf{b}^{(V)} = \mathbf{x}^{(0)}[k]$ is added to the Shared Database.
end

where $\mathcal{U} = \{0, 1, 2, \dots, U\}$, if a new UE is present, whereas $\mathcal{U} = \{1, 2, \dots, U\}$ otherwise. According to (2), the signal backscattered by the u th UE is $\mathbf{r}^{(u)}[k] = g e^{j\phi^{(u)}[k]} \left(\mathbf{z}^{(u)}[k]\right)^*$, then the signal received by the BS at the k th time interval is given by the contributions from all UEs and can be written as

$$\begin{aligned}
\mathbf{y}[k] &= \sum_{u \in \mathcal{U}} \left(\mathbf{H}^{(u)}\right)^T \mathbf{r}^{(u)}[k] + \mathbf{w}[k] \\
&= \sum_{u \in \mathcal{U}} e^{j\phi^{(u)}[k]} \left(\mathbf{H}^{(u)}\right)^T \left(\mathbf{H}^{(u)}\right)^* \sum_{l=0}^V g \sqrt{P^{(l)}} \left(\mathbf{x}^{(l)}[k-1]\right)^* + \mathbf{n}[k] \\
&= \sum_{u \in \mathcal{U}} e^{j\phi^{(u)}[k]} \left(\mathbf{A}^{(u)}\right)^* \sum_{l=0}^V \sqrt{P^{(l)}} \left(\mathbf{x}^{(l)}[k-1]\right)^* + \mathbf{n}[k]
\end{aligned} \tag{14}$$

where $\mathbf{A}^{(0)} = g \left(\mathbf{H}^{(0)}\right)^\dagger \mathbf{H}^{(0)}$, $\mathbf{n}[k] = \mathbf{w}[k] + \sum_{u \in \mathcal{U}} \left(\mathbf{H}^{(u)}\right)^T \left(\boldsymbol{\eta}^{(u)}[k]\right)^*$ and $\{\phi^{(u)}[k]\}$ is the data packet of the u th active UE. All the tasks have access to the received vector $\mathbf{y}[k]$.

The scope of the Shared Database, containing the all the estimated beamforming vectors $\mathbf{B} = \{\mathbf{b}^{(1)}, \mathbf{b}^{(2)}, \dots, \mathbf{b}^{(V)}\}$ of the packets currently under decoding, is two-fold: (i) the v th beamforming vector $\mathbf{b}^{(v)}$ is used by the v th Communication Task to address the UE with index $u = f(v)$ until the end of the corresponding packet; (ii) the set of beamforming vectors in \mathbf{B} is used by the Scouting Task to perform the estimation of the beamforming vector of a possibly newly transmitting UE in a subspace orthogonal to that spanned by the vectors in \mathbf{B} (i.e., in the null space of \mathbf{B}). The latter ensures that the vectors in \mathbf{B} are orthogonal and hence all the tasks (Scouting and Communication) address orthogonal subspaces.

A. Scouting Task

The pseudo-code of the algorithm running on the Scouting Task is reported in Algorithm 1. At the startup time $k = 0$, $\mathbf{x}^{(0)}[0]$ is initialized with a unitary norm random vector. At the $k - 1$ th iteration, with $k > 1$, the Scouting Task Algorithm (see 1) sends the current estimated beamforming vector, $\mathbf{x}^{(0)}[k - 1]$, and receives back the response at time interval k from the new UE (if any) according to (14). Before further processing, the received vector $\mathbf{y}[k]$ is made orthogonal to \mathbf{B} , that is,

$$\hat{\mathbf{y}}[k] = (\mathbf{I} - \mathbf{B}\mathbf{B}^\dagger) \mathbf{y}[k] \quad (15)$$

in order to force the searching in the null space of \mathbf{B} and hence not interfere with the currently active Communication Tasks. Then, a normalized and conjugated version of $\hat{\mathbf{y}}[k]$ is computed and used as the updated beamforming vector $\mathbf{x}^{(0)}[k]$ in the subsequent iteration. The processing operated by Algorithm 1 is the modification of the well-known *Power Method* [33] that, in the absence of noise, interference, and the orthogonalization in (15), allows the estimation of the top-eigenvector of the square matrix $\mathbf{A} = \sum_{u \in \mathcal{U}} \mathbf{A}^{(u)}$. Here, differently from the classical Power Method, due to (15), the matrix seen by the iterative method is $\hat{\mathbf{A}} = (\mathbf{I} - \mathbf{B}\mathbf{B}^\dagger) \mathbf{A}$, which determines the subspace under exploration by the Scouting Task, whose eigenvectors and eigenvalues are denoted by $\{\hat{\lambda}_1, \hat{\lambda}_2, \dots, \hat{\lambda}_{\hat{r}}\}$ and $\{\hat{\mathbf{v}}_1, \hat{\mathbf{v}}_2, \dots, \hat{\mathbf{v}}_{\hat{r}}\}$, respectively, where $\hat{r} = \text{rank}(\hat{\mathbf{A}})$. Moreover, every time a change is operated in \mathbf{B} (addition or removal of elements), $\mathbf{x}^{(0)}[k]$ is reinitiated by drawing a random vector subsequently made orthogonal to the vectors in \mathbf{B} , as in (15), and unitary. In particular, the beamforming vector is updated according to

$$\mathbf{x}^{(0)}[k] = \frac{\hat{\mathbf{y}}^*[k]}{\|\hat{\mathbf{y}}[k]\|} \quad (16)$$

until a change on \mathbf{B} occurs or a new packet is detected. In the absence of noise and interference, after a few iterations, the Power Method ensures that the direction of $\mathbf{x}^{(0)}[k]$ converges to that of the dominant eigenvector $\hat{\mathbf{v}}_1$ of $\hat{\mathbf{A}}$ [33]. The convergence behavior of (16) in the presence of noise will be analyzed later.

Obviously, the new UE can be detected only if $\hat{\mathbf{A}}$ and $\mathbf{A}^{(0)}$ share a not null subspace. It has to be remarked that, in general, it is not guaranteed that $\hat{\mathbf{v}}_1$ is referred to as the channel between the BS and the new UE. In fact, when the UE and BS are in radiating near-field conditions, or in far-field in the presence of multipath, the channel might have a rank larger than one and the same UE can be reached addressing different orthogonal subspaces [42]. In such cases, the

Scouting Task is likely to converge to a subspace related to an UE already under decoding but not yet included in \mathbf{B} , and hence a second Communication Task will be associated with that UE. Duplicated packet decoding is not an issue as it can be easily solved by higher protocol layers. On the contrary, such a phenomenon might be beneficial as it creates a sort of eigenvector diversity. If the packet generation of the new UE is not simultaneous (at symbol time T level) to the generation of an already serving UE, it is likely that all the significative secondary eigenvectors of $\hat{\mathbf{A}}$ have been already removed when the new UE starts its transmission, and $\mathbf{v}_1^{(0)}$ is effectively associated with the new UE, as we will assume in the rest of the paper.

Finally, denote with k^* the time instant a new UE starts the transmission of a packet. The new packet is detected when the SNR $\gamma[k] = \|\hat{\mathbf{y}}[k]\|^2 / \sigma^2$, with $k > k^*$, satisfies $\gamma[k] > \gamma_{\text{dec}}$ and $\gamma[k] / \gamma[k-1] < \gamma_{\Delta}$. The first inequality checks that a certain level of energy has been received compared to the noise level, whereas the second one guarantees that (16) is close to the convergence, with the thresholds γ_{dec} and γ_{Δ} to be properly tuned.

B. Communication Task

Once a new packet has been detected by the Scouting Task, a new Communication Task is activated whose algorithm is reported in Algorithm 2. Denote with $k^{(v)}$ the time instant the packet is detected by the Scouting Task and the Communication Tasks starts, being v the index associated to the new packet generated by the u th UE, with $u = f(v)$, and with $\mathbf{b}^{(v)} = \mathbf{x}^{(0)} [k^{(v)}]$ the corresponding beamforming vector estimated through Algorithm 1 and stored in the Shared Database by the Scouting Task. The Communication Task, for $k \geq k^{(v)}$ until the end of the packet, executes Algorithm 2 which, at each iteration, always transmits the same beamforming vector $\sqrt{P^{(v)}} \mathbf{x}^{(v)} [k-1]$, with $\mathbf{x}^{(v)} [k-1] = \mathbf{b}^{(v)}$. Subsequently, according to (8) and (14), the decision variable is formed as

$$\begin{aligned}
u^{(v)}[k] &= \left(\mathbf{b}^{(v)}\right)^{\dagger} \mathbf{y}^*[k] \\
&= \sum_{i \in \mathcal{U}} e^{-j\phi^{(i)}[k]} \left(\mathbf{b}^{(v)}\right)^{\dagger} \mathbf{A}^{(u)} \sum_{l=0}^V \sqrt{P^{(l)}} \mathbf{x}^{(l)}[k-1] + \left(\mathbf{b}^{(v)}\right)^{\dagger} \mathbf{n}^*[k] \\
&= e^{-j\phi^{(u)}[k]} \sum_{l=0}^V \sqrt{P^{(l)}} \left(\mathbf{b}^{(v)}\right)^{\dagger} \mathbf{A}^{(u)} \mathbf{x}^{(l)}[k-1] \\
&\quad + \sum_{i \in \mathcal{U}, i \neq u} e^{-j\phi^{(i)}[k]} \sum_{l=0}^V \sqrt{P^{(l)}} \left(\mathbf{b}^{(v)}\right)^{\dagger} \mathbf{A}^{(u)} \mathbf{x}^{(l)}[k-1] + \left(\mathbf{b}^{(v)}\right)^{\dagger} \mathbf{n}^*[k]. \quad (17)
\end{aligned}$$

Algorithm 2: Algorithm of the v th Communication Task.

```

Initialization: active = 1, k = k(v) // k(v) time instant of packet detection
while active=1 do
    transmit:  $\sqrt{P^{(v)}} \mathbf{x}^{(v)}[k-1] = \sqrt{P^{(v)}} \mathbf{b}^{(v)}$  //
    receive:  $\mathbf{y}[k]$  //
     $u^{(v)}[k] = (\mathbf{b}^{(v)})^\dagger \mathbf{y}^*[k]$  // decision variable
     $\hat{\phi}[k] = \text{demodulation}(-\arg\{u^{(v)}[k]\})$  // data demodulation
     $\gamma[k] = |u^{(v)}[k]|^2 / \sigma^2$  // SNR computation
    If  $\gamma[k] < \gamma_{\text{drop}}$ , then beamforming vector  $\mathbf{b}^{(v)}$  is removed from the Shared Database and this task is
    de-instantiated (active = 0, V = V - 1) //
    k = k + 1;
end

```

A decision on the transmitted phase $\phi^{(u)}[k]$ from the UE with index $u = f(v)$ is made based on the argument of $u^{(v)}[k]$ in (17) according to the mapping scheme considered, as explained in Sec. III. The first term in (17) is the useful term. Equation (17) reveals that, in general, the decision variable is affected by the presence of interference from other UEs (second term), caused by eventual not orthogonality of the users' channels, and thermal noise (third term). Finally, when $\gamma[k] = |u^{(v)}[k]|^2 / \sigma^2 < \gamma_{\text{drop}}$, the end of the packet has been likely reached, and the task is deactivated.

C. Orthogonal Channels (favorable propagation)

Equation (17) shows that, depending on channel characteristics, the decision variable might be deteriorated by the presence of inter-user interference. In this section, we investigate the particular but significant scenario where the favorable propagation condition is met, which is typical when employing a massive number of antenna elements at the BS [43].

Consider the scenario in which the subspaces spanned by $\mathbf{H}^{(u)}$ are orthogonal to each other, and so those by $\mathbf{A}^{(u)}$, for $u \in \mathcal{U}$. This implies that $(\mathbf{v}_n^{(v)})^\dagger \mathbf{A}^{(u)} \mathbf{v}_m^{(l)}$ is different from zero only when $v = l$ and $m = n$. This assumption can be in general approached when UEs are located in different positions and a large number of antennas is used at the BS. This condition is typically referred to as *favorable propagation* in massive MIMO literature. For instance, in [29] it has been shown that the favorable propagation condition can be approached even in correlated Rayleigh and geometry-based multi-user MIMO channels when N grows.

Under favorable propagation and supposing an accurate estimate of the eigenvectors has been reached by the Scouting Task so that $\mathbf{b}^{(v)} \simeq \mathbf{v}_i^{(u)}$, with $u = f(v)$, for some $i \in \{1, 2, \dots, r^{(u)}\}$,

the inter-user interference terms become negligible and (17) simplifies to

$$\mathbf{u}^{(v)}[k] \simeq \sqrt{P_T} e^{-j\phi^{(u)}[k]} \left(\mathbf{b}^{(v)} \right)^\dagger \mathbf{A}^{(u)} \mathbf{b}^{(v)} + \left(\mathbf{b}^{(v)} \right)^\dagger \mathbf{n}^*[k] \simeq \sqrt{P_T} \lambda_i^{(u)} e^{-j\phi^{(u)}[k]} + n_i[k] \quad (18)$$

like in the single-user case in (9) because $\mathbf{b}^{(v)}$ is an eigenvector of the round-trip time channel matrix $\mathbf{A}^{(u)}$. In addition, $\mathring{\mathbf{A}} = \mathbf{A}^{(0)}$ and $\mathring{\mathbf{v}}_1 = \mathbf{v}_1^{(0)}$, that is, the top-eigenvector of $\mathbf{A}^{(0)}$.

V. CONVERGENCE ANALYSIS OF THE SCOUTING TASK

The convergence behavior of the Scouting Task, given a new UE started its transmission, can be analyzed assuming that no other UE starts its transmission during the first symbols of the packet and/or has its channel subspace partially overlapped in the subspace spanned by $\mathring{\mathbf{A}}$. In the presence of noise, (16) reads

$$\mathbf{x}^{(0)}[k] = \frac{\mathring{\mathbf{y}}^*[k]}{\|\mathring{\mathbf{y}}[k]\|} = \frac{\sqrt{P_{\text{scout}}} \mathring{\mathbf{A}} e^{-j\phi[k]} \mathbf{x}^{(0)}[k-1] + \mathbf{n}[k]}{\|\sqrt{P_{\text{scout}}} \mathring{\mathbf{A}} e^{-j\phi[k]} \mathbf{x}^{(0)}[k-1] + \mathbf{n}[k]\|} \quad (19)$$

where

$$\mathring{\mathbf{y}}^*[k] = \sum_{j=1}^N \mathring{\mathbf{v}}_j \left(\sqrt{P_{\text{scout}}} \mathring{\lambda}_j x_j[k-1] e^{-j\phi[k]} + n_j[k] \right) \quad (20)$$

and $x_j[k], n_j[k] \sim \mathcal{CN}(0, \sigma^2)$ represent, respectively, the projections of $\mathbf{x}^{(0)}[k], \mathbf{n}[k]$ onto $\mathring{\mathbf{v}}_j$. Note that the term carrying the information (i.e., the phase $\phi[k]$) also includes the noise from the previous iterations, which is contained in $x_j[k-1]$. Moreover, $|x_j[k-1]|^2 / \|\mathbf{x}^{(0)}[k-1]\|^2 = |x_j[k-1]|^2$, being $\|\mathbf{x}^{(0)}[k]\|^2 = 1$, represents the fraction of the total transmitted power (useful plus noise) associated to direction $\mathring{\mathbf{v}}_j$ at the discrete time $k-1$. Then, at the end of the k th time interval, the received SNR along the direction $\mathring{\mathbf{v}}_j$ is given by

$$\text{SNR}_j[k] = \frac{P_{\text{scout}} \mathring{\lambda}_j^2 |x_j[k-1]|^2}{\sigma^2}. \quad (21)$$

The goal is to determine an iterative expression for $\text{SNR}_j[k]$, which drives the signal demodulation performance in the Communication Task, and evaluate the convergence condition of the Scouting Task we proposed. Considering (20), the fraction of the total power that is associated with direction $\mathring{\mathbf{v}}_j$ at the beginning of time interval k can be written as

$$|x_j[k]|^2 = \frac{P_{\text{scout}} \mathring{\lambda}_j^2 |x_j[k-1]|^2 + \sigma^2}{\sum_{i=1}^N \left(P_{\text{scout}} \mathring{\lambda}_i^2 |x_i[k-1]|^2 + \sigma^2 \right)}. \quad (22)$$

By inverting (21) and plugging $|x_j[k]|^2$ at both the left-hand and right-hand sides of (22), we obtain the following iterative formula for $\text{SNR}_j[k]$

$$\begin{aligned}\text{SNR}_j[k] &= \frac{P_{\text{scout}} \hat{\lambda}_j^2 (\text{SNR}_j[k-1] + 1)}{\sigma^2 [\sum_{i=1}^N (\text{SNR}_i[k-1] + 1)]} \\ &= \text{SNR}_j^{(\text{max})} \frac{\text{SNR}_j[k-1] + 1}{N + \sum_{i=1}^p \text{SNR}_i[k-1]}\end{aligned}\quad (23)$$

for $j = 1, 2, \dots, \hat{r}$, and $k \geq k^*$, where $\text{SNR}_j[k^*] = \text{SNR}_j^{(\text{max})} |x_j[k^*]|^2$, and

$$\text{SNR}_j^{(\text{max})} = \frac{P_{\text{scout}} \hat{\lambda}_j^2}{\sigma^2}\quad (24)$$

representing the maximum SNR along the direction $\hat{\mathbf{v}}_j$, i.e., the SNR one would obtain if all the power was concentrated to direction $\hat{\mathbf{v}}_j$. Note that if $\mathbf{x}[k^*]$ is initialized randomly, then $|x_j[k^*]|^2 \simeq 1/N$ so that $\text{SNR}_j[k^*] \simeq \text{SNR}_j^{(\text{max})}/N$.

In the particular but common case where channel $\hat{\mathbf{A}}$ has rank 1, the SNR at the k th time instant along direction $\hat{\mathbf{v}}_1$ in (23) simplifies into

$$\text{SNR}_1[k] = \text{SNR}_1^{(\text{max})} \frac{\text{SNR}_1[k-1] + 1}{N + \text{SNR}_1[k-1]}\quad (25)$$

for $k \geq k^*$, which allows an easy evaluation of the convergence value. At the convergence it must be $\text{SNR}_1[k] \simeq \text{SNR}_1[k-1]$ then, by dropping the time index, (25) becomes the quadratic equation

$$\text{SNR}_1 = \text{SNR}_1^{(\text{max})} \frac{\text{SNR}_1 + 1}{N + \text{SNR}_1}\quad (26)$$

whose positive solution is

$$\text{SNR}_1 = \frac{1}{2} \left(N - \text{SNR}_1^{(\text{max})} + \left| \text{SNR}_1^{(\text{max})} - N \right| \sqrt{1 + \frac{\text{SNR}_1^{(\text{max})}}{(\text{SNR}_1^{(\text{max})} - N)^2}} \right).\quad (27)$$

Denote with $\text{SNR}_1^{(\text{boot})} = \text{SNR}_1^{(\text{max})}/N$ the *bootstrap SNR*. By inspection of (27) it can easily verified that if $\text{SNR}_1^{(\text{boot})} \gg 1$, then at the convergence it is $\text{SNR}_1 \simeq \text{SNR}_1^{(\text{max})} - N \simeq \text{SNR}_1^{(\text{max})} \gg 1$, which takes the role of asymptotic SNR corresponding to the optimum beamforming vector for a channel with rank 1. When the bootstrap SNR is much less than one, we still have convergence but at $\text{SNR}_1 \ll 1$ so that the link cannot be established. It is worth noticing that the convergence value does not depend on the initial random guess, but only

on the bootstrap SNR. According to (11), the link budget can be ameliorated by increasing M and/or N indifferently as both play quadratically. On the contrary, the bootstrap SNR increases quadratically with M but only linearly with N , therefore it is better to increase M than N , when possible. The convergence analysis for $\hat{r} > 1$ involves the evaluation of an $\hat{r} + 1$ polynomial equation that becomes not feasible analytically for large r . Despite that, numerical investigations reported in the next section put in evidence that the previous condition to reach the asymptotic SNR holds even when $\hat{r} > 1$ so that, upon convergence, $|x_1[k]| \gg |x_j[k]|$ for $j > 1$.

When the Scouting Task detects the new UE, let's say at time interval \tilde{k} , $\mathbf{x}^{(0)}[\tilde{k}]$ is used as an estimate of the top-eigenvector $\hat{\mathbf{v}}_1$ in the Communication Task that will be associated to the UE. Such an estimate is characterized by $\text{SNR}_1[\tilde{k}]$ that can be computed through the iterative formula (23). The decision variable $u[k]$ at the k th symbol is proportional to the product

$$u[k] \propto \mathbf{x}^\dagger[\tilde{k}] \mathbf{y}^*[k] = \sqrt{P_T} e^{-j\phi[k]} \sum_{j=1}^{\hat{r}} \lambda_j |x_j[\tilde{k}]|^2 + \mathbf{x}^\dagger[\tilde{k}] \mathbf{n}[k] \quad (28)$$

in which the first term is the useful one, as it contains the phase $\phi[k]$ that carries the information, and the second term represents the noise. Since $\|\mathbf{x}[\tilde{k}]\|^2 = 1$, the SNR at the input of the detector is

$$\text{SNR}^{(\text{dec})} = \frac{P_T \left(\sum_{j=1}^{\hat{r}} \lambda_j |x_j[\tilde{k}]|^2 \right)^2}{\sigma^2}. \quad (29)$$

Therefore, we can rewrite (29) as a function of $\text{SNR}_j[k]$ as

$$\text{SNR}^{(\text{dec})} = \frac{P_T}{P_{\text{scout}}} \left(\sum_{j=1}^{\hat{r}} \frac{\text{SNR}_j[\tilde{k}]}{\sqrt{\text{SNR}_j^{(\text{max})}}} \right)^2 \simeq \frac{P_T}{P_{\text{scout}}} \text{SNR}_1^{(\text{max})} = \frac{P_T \lambda_1^2}{\sigma^2}. \quad (30)$$

In case of favorable propagation it is

$$\text{SNR}^{(\text{dec})} \simeq \frac{P_T \left(\lambda_1^{(0)} \right)^2}{\sigma^2} \quad (31)$$

which resembles (10) of the single-user scenario.

VI. NUMERICAL RESULTS

In this section, we report some simulation results with the purpose to investigate the performance of the proposed scheme. The values of the system parameters adopted for the analysis

TABLE I
PARAMETERS USED IN THE ANALYSIS AND THE SIMULATION

Parameter	Symbol	Value
Carrier frequency	f_c	100 GHz
BS antenna element gain	G_{BS}	0 dB (isotropic)
SCM single cell gain	G_{SCM}	0 dB (isotropic)
SCM backscatter gain	g	20 dB
Bandwidth	W	10 MHz
Symbol time	T	100 ns
TX power	P_T	-5 dBm
Power boost scouting	P_{scout}/P_T	10 dB
SCM cell noise figure	F_{SCM}	3 dB
BS noise figure	F_{BS}	3 dB
BS antenna elements	N	30×30 (4.5×4.5 cm ² planar array)
SCM cells per user	M	20×20 (3×3 cm ² planar array)
Path-loss exponent	β	2 (free-space/LOS), 2.5 (NLOS)
Detection SNR threshold	γ_{dec}	30 dB
Drop SNR threshold	γ_{drop}	5 dB
Delta SNR convergence	γ_{Δ}	5 dB
Packet length	K	144 bits
Guard symbols	K_g	16 bits
Packet duration	$T_p = KT$	14.4 μ s

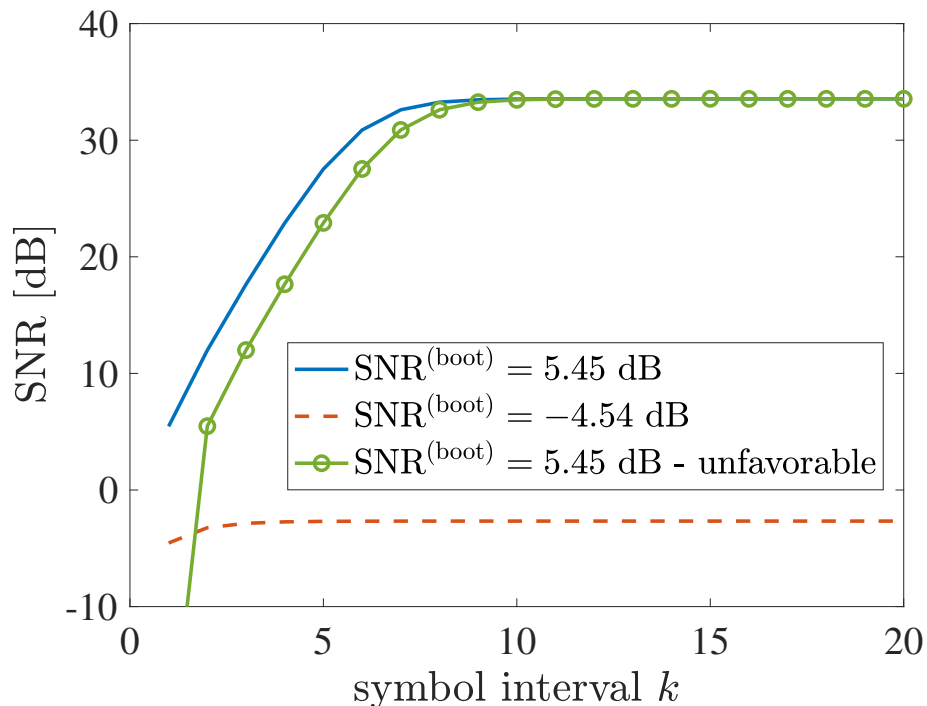


Fig. 4. Time evolution of $SNR_1[k]$ during the Scouting Task for different bootstrap conditions in the case of a rank-1 channel.

and the simulations are reported in Table I, if not otherwise specified. The scenario considered is composed of a BS, equipped with a planar array deployed along the xy -plane, located at

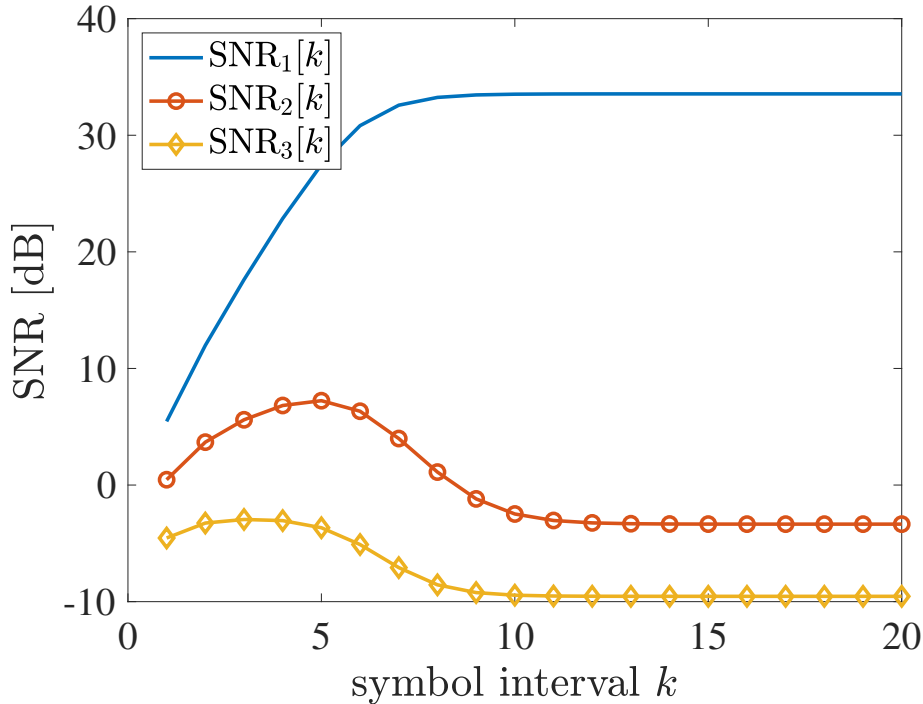


Fig. 5. Time evolution of $\text{SNR}_j[k]$ during the Scouting Task in the case of a rank-3 channel.

$(0, 0, 0)$ [m], and UEs generating very short packets of total length $K = 144$ bits (32 bytes payload). In particular, the packets are generated randomly with exponentially distributed inter-arrival time with mean μ [s], corresponding to a total offered traffic $G = T_p/\mu$, where $T_p = K T$ is the packet duration. Each packet corresponds to an UE whose position is generated randomly with uniform distribution within the area centered in $(0, 0, 10)$ [m] and size 10×10 [m²]. The UE's SCMs are supposed to lay on the xy -plane.

In Fig. 4, the time evolution of $\text{SNR}_1[k]$ during the Scouting Task is shown for different bootstrap conditions in the case of rank-1 channel computed using the iterative equation (23), with $k^* = 1$. In the first 2 plots, a random initial guess of the beamforming vector, corresponding to $\text{SNR}_1[1] \approx \text{SNR}_1^{(\max)}/N$, was assumed, whereas the third plot is related to an even more unfavorable situation where $\text{SNR}_1[1] = \text{SNR}_1^{(\max)}/N^2$. The blue and green curves have been evaluated with $\text{SNR}_1^{(\max)} = 35$ dB and $\text{SNR}_1^{(\max)} = 25$ dB, respectively, to which a bootstrap SNR of 5.45 dB and -4.54 dB correspond. It can be noticed that when the bootstrap SNR is larger than one, the SNR converges after a few steps to $\text{SNR}_1^{(\max)}$ and the packet can be detected, whereas it converges to very low SNR values when the bootstrap SNR is less than one, as predicted by

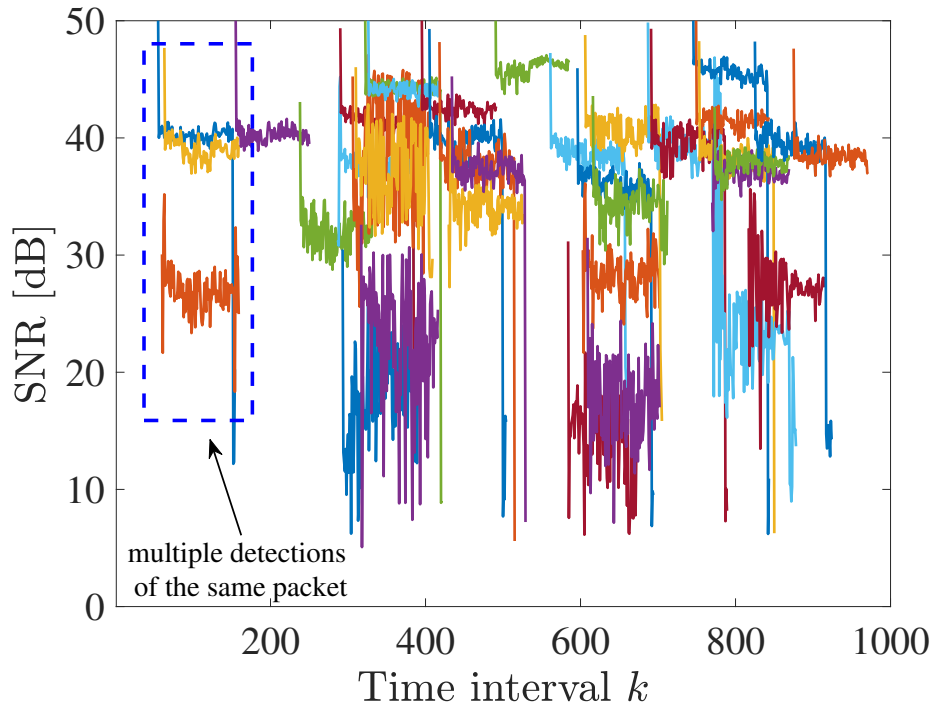


Fig. 6. Example of SNR evolution during the Communication Tasks with $G = 2$. Different colors refers to different packets/UEs managed by different Communication Tasks.

(27). From Fig. 4, it can also be concluded that the impact of the initial beamforming vector on the SNR evolution is marginal and it does not affect the final value.

The situation with a rank-3 channel is analyzed in Fig. 5 where the evolution of $\text{SNR}_j[k]$, $j = 1, 2, 3$, is plotted for $\text{SNR}_1^{(\max)} = 35$ dB, 30 dB, and 25 dB. The proposed iterative method ensures the convergence to the top eigenvector of the channel, as can be appreciated in the figure (blue curve). Comparing the blue curves in Figs. 4 and 5, it can also be observed that the convergence speed to the top-eigenvector is only slightly affected by the rank of the channel. In all cases, the convergence time is below 10 time intervals. This suggests that a guard time of $K_g = 16$ symbols set to zero, inserted at the beginning of each packet and followed by the payload of 32 bytes, gives sufficient time to the Scouting Task to converge and detect the packet.

An example of realization of the SNR evolution in a time frame of 1000 symbols is shown in Fig. 6 for an offered traffic of $G = 2$ in free-space condition. In particular, the SNR evolution during the Communication Task of each detected packet, identified by a different color, is plotted. The SNR fluctuations are mainly due to the inter-user interference because the channels are not

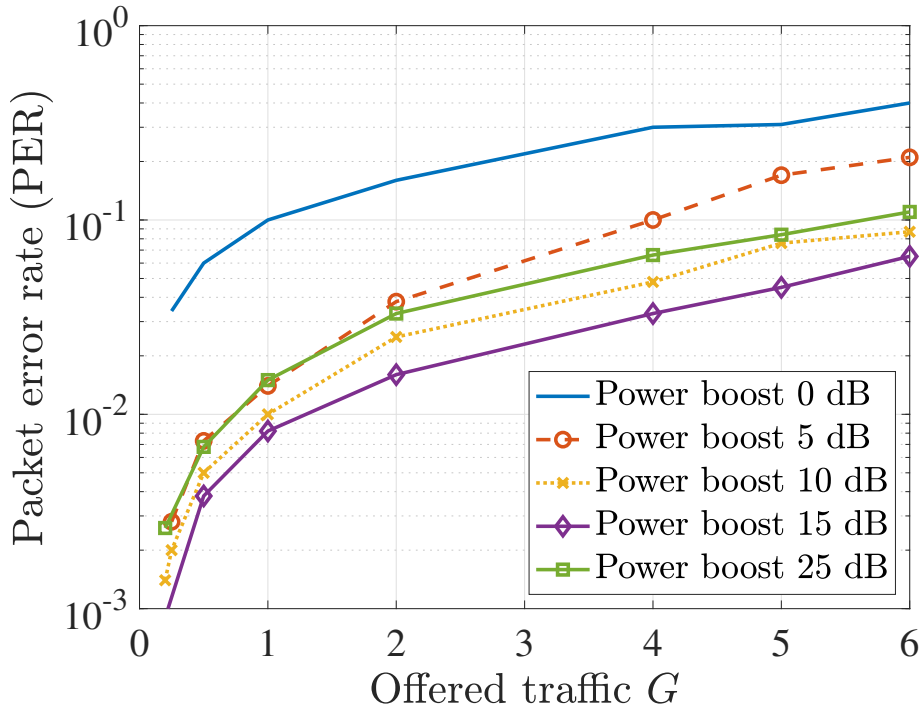


Fig. 7. Packet error rate as a function of the offered traffic G . Effect of Scouting Task power boost. Free space condition. $P_T = -5$ dBm.

orthogonal, i.e., the favorable propagation condition is not met. As it can be seen, despite most of the transmissions are overlapped, the scheme is capable of resolving them in an efficient manner. Different SNRs are due to different path loss values (UEs' positions) and inter-user interference caused by partial channels subspaces overlap, whereas the first peak is the residual of the power boost during the last scouting symbol. Highlighted with a blue rectangle are multiple successful detections of the same packet by different Communication Tasks using different estimated eigenvectors. Such a situation is representative of a near-field channel condition for the associated UE.

In Fig. 7, the packet error rate (PER), corresponding to $1 - \{\text{Probability of packet detection}\}$, as a function of the offered traffic G is shown for different power boost levels in free space. The PER has been computed through Monte Carlo simulations terminated when at least 100 erroneous packets were counted. It can be noticed that the power boost is in general beneficial but also that a compromise has to be found also avoiding too much higher values. In fact, while an increase of the power boost facilitates the detection of new packets by the Scouting Task, on the other hand, it might increase the interference to the packets already under decoding in the

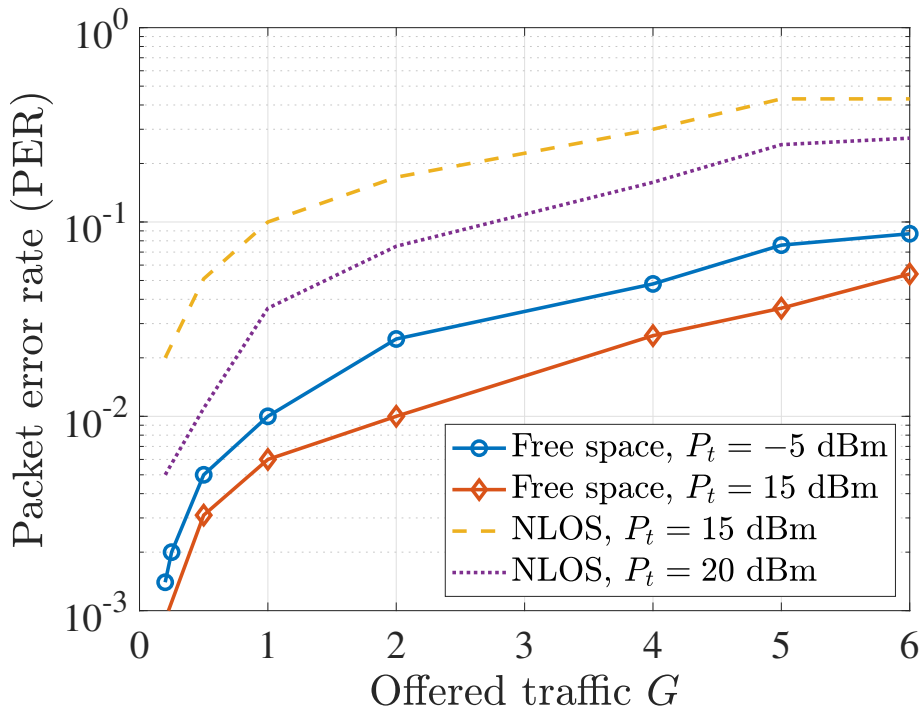


Fig. 8. Packet error rate as a function of the offered traffic G for different transmitted power levels and channel models. Power boost 10 dB.

absence of favorable propagation. Simulations evidenced that 15 dB provides the lowest PER in all cases, but the performance is still good with a lower level of 10 dB that is considered in the next plots. Obviously, under favorable propagation (massive MIMO) the inter-user interference is minimized and the determination of the power boost is less critical.

The impact of the transmitted power and channel models can be observed in Fig. 8. In particular, free-space and the NLOS CDL-C multipath 3GPP channel models [44] with a delay spread of 9 ns have been considered. Obviously, higher transmitted power levels are necessary in NLOS condition due to the more severe path loss. The increase of the transmitted power lowers slightly the PER indicating that the performance is mainly limited by the inter-user interference. Achieving favorable propagation through a substantial increase of the antenna elements at the BS is one possible solution to mitigate or even eliminate the inter-user interference. Future investigations will be oriented to approaches based on successive interference cancellation schemes exploiting the packet diversity obtained in near-field conditions where the same packet is likely received associated with different eigenvectors. Another line of investigation is to combine the proposed scheme with coded random access schemes [26] to further increase the reliability.

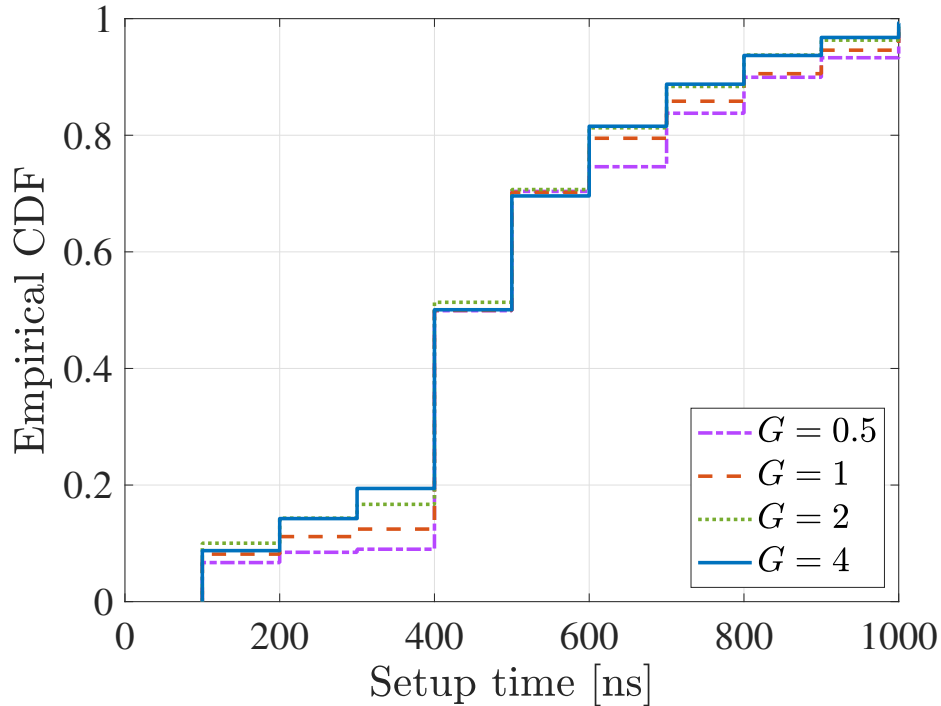


Fig. 9. Empirical CDF of the set up time for different values of the offered traffic. Free-space condition.

Finally, Fig. 9 shows the empirical CDF of the set-up time distribution of successfully detected and decoded packets, i.e., the convergence time of the Scouting Task, for different values of the offered traffic. As it can be noticed, the impact of the offered traffic is marginal and the values are extremely low, below $1 \mu s$, corresponding to 10 symbols. It is worth noting that successfully decoded packets are subject to neither jitter nor latency as each packet is available at the BS as soon as the last bit has been transmitted and received, i.e., within the symbol time T .

From the computational complexity point of view, the complexity of the proposed scheme is proportional to the number of parallel active Communication Tasks which, in turn, depends on the offered traffic. Both the Scouting and Communication Tasks involve elementary operations whose number is proportional to the number N of antennas at the BS but not to the number of cells M at the SCM. Therefore, M can be considered as a useful degree of freedom that can be exploited to improve the link budget, and hence the $\text{SNR}^{(\text{boot})}$, without any drawback in terms of algorithm's complexity.

VII. CONCLUSION

In this paper, we have proposed the adoption of modulating SCMs as a means to realize ultra-low complexity grant-free MIMO communications exploiting retro-directive backscattering. Thanks to the iterative algorithm introduced in this paper, inspired by the Power Method, the BS can estimate the optimal beamforming vector for the BS-UE round-trip channel and hence establish the optimal single-layer MIMO communication. Numerical results have put in evidence that MIMO communications can be established after a few iterations, with μs -level setup time and almost zero latency and jitter, even using very large arrays and in the presence of realistic channels characterized by multipath. The proposed system is particularly appealing in many applications envisioned for 6G requiring low-complexity MIMO solutions at high frequencies such as IIoT.

REFERENCES

- [1] S. R. Pokhrel, J. Ding, J. Park, O.-S. Park, and J. Choi, "Towards enabling critical mMTC: A Review of URLLC Within mMTC," *IEEE Access*, vol. 8, pp. 131 796–131 813, 2020.
- [2] H. Viswanathan and P. E. Mogensen, "Communications in the 6G Era," *IEEE Access*, vol. 8, pp. 57 063–57 074, 2020.
- [3] Z. Wan, Z. Gao, M. Di Renzo, and L. Hanzo, "The Road to Industry 4.0 and Beyond: A Communications-, Information-, and Operation Technology Collaboration Perspective," *arXiv e-prints*, p. arXiv:2205.04741, May 2022.
- [4] A. Costanzo, D. Dardari, J. Aleksandravicius, N. Decarli, M. D. Prete, D. Fabbri, M. Fantuzzi, A. Guerra, D. Masotti, M. Pizzotti, and A. Romani, "Energy autonomous UWB localization," *IEEE Journal of Radio Frequency Identification*, vol. 1, no. 3, pp. 228–244, Sept 2017.
- [5] X. Chen, D. W. K. Ng, W. Yu, E. G. Larsson, N. Al-Dhahir, and R. Schober, "Massive access for 5G and beyond," *IEEE Journal on Selected Areas in Communications*, vol. 39, no. 3, pp. 615–637, March 2021.
- [6] M. Giordani, M. Mezzavilla, and M. Zorzi, "Initial access in 5G mmwave cellular networks," *IEEE Commun. Mag.*, vol. 54, no. 11, pp. 40–47, Nov. 2016.
- [7] S.-W. Qu, H. Yi, B. J. Chen, K. B. Ng, and C. H. Chan, "Terahertz reflecting and transmitting metasurfaces," *Proceedings of the IEEE*, vol. 105, no. 6, pp. 1166–1184, 2017.
- [8] M. Barbuto, Z. Hamzavi-Zarghani, M. Longhi, A. Monti, D. Ramaccia, S. Vellucci, A. Toscano, and F. Bilotti, "Metasurfaces 3.0: a new paradigm for enabling smart electromagnetic environments," *IEEE Transactions on Antennas and Propagation*, pp. 1–1, 2021.
- [9] M. D. Renzo, A. Zappone, M. Debbah, M. Alouini, C. Yuen, J. D. Rosny, and S. Tretyakov, "Smart radio environments empowered by reconfigurable intelligent surfaces: How it works, state of research, and road ahead," *IEEE Journal on Selected Areas in Communications*, pp. 1–1, 2020.
- [10] M. Faenzi, G. Minatti, D. González-Ovejero, F. Caminita, E. Martini, C. D. Giovampaola, and S. Maci, "Metasurface antennas: New models, applications and realizations," *Scientific Reports*, vol. 9, no. 10178, pp. 1–14, 2019.
- [11] P. Mursia, V. Sciancalepore, A. Garcia-Saavedra, L. Cottatellucci, X. C. Perez, and D. Gesbert, "RISMA: Reconfigurable intelligent surfaces enabling beamforming for IoT massive access," *IEEE Journal on Selected Areas in Communications*, vol. 39, no. 4, pp. 1072–1085, April 2021.

- [12] D. Dardari and N. Decarli, "Holographic communication using intelligent surfaces," *IEEE Communications Magazine*, vol. 59, no. 6, pp. 35–41, June 2021.
- [13] D. Dardari and D. Massari, "Using metaprisms for performance improvement in wireless communications," *IEEE Transactions on Wireless Communications*, vol. 20, no. 5, pp. 3295–3307, May 2021.
- [14] A. Abrardo, D. Dardari, and M. Di Renzo, "Intelligent reflecting surfaces: Sum-rate optimization based on statistical position information," *IEEE Transactions on Communications*, vol. 69, no. 10, pp. 7121–7136, Oct 2021.
- [15] J. Hu, H. Zhang, B. Di, K. Bian, and L. Song, "Meta-IoT: Simultaneous sensing and transmission by meta-material sensor based internet of things," *IEEE Transactions on Wireless Communications*, pp. 1–1, 2022.
- [16] H. Ding, M.-S. Alouini, K. Xin, H. Li, and S. Xu, "Symbiotic ambient backscatter systems: Outage behavior and ergodic capacity," *IEEE Internet of Things Journal*, pp. 1–1, 2022.
- [17] Y.-C. Liang, Q. Zhang, J. Wang, R. Long, H. Zhou, and G. Yang, "Backscatter communication assisted by reconfigurable intelligent surfaces," *Proceedings of the IEEE*, vol. 110, no. 9, pp. 1339–1357, 2022.
- [18] D. Dardari, R. D'Errico, C. Roblin, A. Sibille, and M. Z. Win, "Ultrawide bandwidth RFID: The next generation?" *Proc. IEEE*, vol. 98, no. 9, pp. 1570–1582, Sep 2010, special Issue on RFID - A Unique Radio Innovation for the 21st Century.
- [19] J.-P. Niu and G. Y. Li, "An overview on backscatter communications," *Journal of Communications and Information Networks*, vol. 4, no. 2, pp. 1–14, 2019.
- [20] S. Taravati and G. V. Eleftheriades, "Programmable nonreciprocal meta-prism," *Scientific Reports*, vol. 11, no. 1, p. 7377, 2021. [Online]. Available: <https://doi.org/10.1038/s41598-021-86597-1>
- [21] A. Silva, F. Monticone, G. Castaldi, V. Galdi, A. Alù, and N. Engheta, "Performing mathematical operations with metamaterials," *Science*, vol. 343, no. 6167, pp. 160–163, 2014. [Online]. Available: <https://science.sciencemag.org/content/343/6167/160>
- [22] R. Miyamoto and T. Itoh, "Retrodirective arrays for wireless communications," *IEEE Microwave Magazine*, vol. 3, no. 1, pp. 71–79, 2002.
- [23] D. Dardari, M. Lotti, N. Decarli, and G. Pasolini, "Establishing MIMO communications automatically using self-conjugating metasurfaces," in *ICC 2023*, Nov. 2023, submitted.
- [24] L. Liu and W. Yu, "Massive connectivity with massive MIMO - Part I: Device activity detection and channel estimation," *IEEE Transactions on Signal Processing*, vol. 66, no. 11, pp. 2933–2946, June 2018.
- [25] L. Liu, E. G. Larsson, W. Yu, P. Popovski, C. Stefanovic, and E. de Carvalho, "Sparse signal processing for grant-free massive connectivity: A future paradigm for random access protocols in the internet of things," *IEEE Signal Processing Magazine*, vol. 35, no. 5, pp. 88–99, Sep. 2018.
- [26] E. Paolini, C. Stefanovic, G. Liva, and P. Popovski, "Coded random access: applying codes on graphs to design random access protocols," *IEEE Communications Magazine*, vol. 53, no. 6, pp. 144–150, June 2015.
- [27] L. Yang, P. Fan, L. Li, Z. Ding, and L. Hao, "Grant-Free Transmission by LDPC Matrix Mapping and Integrated Cover-MPA Detector," *arXiv e-prints*, p. arXiv:2207.00272, Jul. 2022.
- [28] M. Mohammadkarimi, O. A. Dobre, and M. Z. Win, "Massive uncoordinated multiple access for beyond 5G," *IEEE Transactions on Wireless Communications*, vol. 21, no. 5, pp. 2969–2986, May 2022.
- [29] X. Wu and D. Liu, "Novel insight into multi-user channels with multi-antenna users," *IEEE Communications Letters*, vol. 21, no. 9, pp. 1961–1964, 2017.
- [30] X. Xie, Y. Wu, J. An, J. Gao, W. Zhang, C. Xing, K.-K. Wong, and C. Xiao, "Massive unsourced random access: Exploiting angular domain sparsity," *IEEE Transactions on Communications*, vol. 70, no. 4, pp. 2480–2498, 2022.
- [31] A.-S. Bana, G. Xu, E. D. Carvalho, and P. Popovski, "Ultra reliable low latency communications in massive multi-antenna systems," in *2018 52nd Asilomar Conference on Signals, Systems, and Computers*, Oct 2018, pp. 188–192.

- [32] H. Xiu, Z. Gao, A. Liao, Y. Mei, D. Zheng, S. Tan, M. D. Renzo, and L. Hanzo, "Joint activity detection and channel estimation for massive IoT access based on millimeter-wave/terahertz multi-panel massive MIMO," *IEEE Transactions on Vehicular Technology*, pp. 1–6, 2022.
- [33] G. H. Golub and H. A. van der Vorst, "Eigenvalue computation in the 20th century," *Journal of Computational and Applied Mathematics*, vol. 123, no. 1, pp. 35–65, 2000, numerical Analysis 2000. Vol. III: Linear Algebra. [Online]. Available: <https://www.sciencedirect.com/science/article/pii/S0377042700004131>
- [34] J.-F. Bousquet, S. Magierowski, and G. G. Messier, "A 4-GHz active scatterer in 130-nm CMOS for phase sweep amplify-and-forward," *IEEE Transactions on Circuits and Systems I: Regular Papers*, vol. 59, no. 3, pp. 529–540, 2012.
- [35] K. K. Kishor and S. V. Hum, "An amplifying reconfigurable reflectarray antenna," *IEEE Transactions on Antennas and Propagation*, vol. 60, no. 1, pp. 197–205, 2012.
- [36] J. Lončar, A. Grbic, and S. Hrabar, "Ultrathin active polarization-selective metasurface at X-band frequencies," *Phys. Rev. B*, vol. 100, p. 075131, Aug 2019. [Online]. Available: <https://link.aps.org/doi/10.1103/PhysRevB.100.075131>
- [37] Z. Zhang, L. Dai, X. Chen, C. Liu, F. Yang, R. Schober, and H. V. Poor, "Active RIS vs. Passive RIS: Which Will Prevail in 6G?" *arXiv e-prints*, p. arXiv:2103.15154, Mar. 2021.
- [38] C. Allen, K. Leong, and T. Itoh, "A negative reflective/refractive "meta-interface" using a bi-directional phase-conjugating array," in *IEEE MTT-S International Microwave Symposium Digest, 2003*, vol. 3, 2003, pp. 1875–1878 vol.3.
- [39] A. R. Katko, S. Gu, J. P. Barrett, B.-I. Popa, G. Shvets, and S. A. Cummer, "Phase conjugation and negative refraction using nonlinear active metamaterials," *Phys. Rev. Lett.*, vol. 105, p. 123905, Sep 2010.
- [40] M. Kalaagi and D. Seetharamdoo, "Fano resonance based multiple angle retrodirective metasurface," in *2020 14th European Conference on Antennas and Propagation (EuCAP)*, 2020, pp. 1–4.
- [41] E. G. Larsson and P. Stoica, *Space-Time Block Coding for Wireless Communications*. New York, USA: Cambridge Univ. Press, 2003.
- [42] N. Decarli and D. Dardari, "Communication modes with large intelligent surfaces in the near field," *IEEE Access*, vol. 9, pp. 165 648–165 666, 2021.
- [43] E. Björnson, J. Hoydis, and L. Sanguinetti, *Massive MIMO Networks: Spectral, Energy, and Hardware Efficiency*. Vol. 11, No. 3-4, pp. 154–655: IEEE Foundations and Trends in Signal Processing, 2017.
- [44] 3GPP, "Study on channel model for frequencies from 0.5 to 100 GHz (3GPP TR 38.901)," 3GPP, Tech. Rep., 2019.